



UvA-DARE (Digital Academic Repository)

Physiological and genetic studies towards biofuel production in cyanobacteria

Schuurmans, R.M.

Publication date

2017

Document Version

Other version

License

Other

[Link to publication](#)

Citation for published version (APA):

Schuurmans, R. M. (2017). *Physiological and genetic studies towards biofuel production in cyanobacteria*. [Thesis, fully internal, Universiteit van Amsterdam].

General rights

It is not permitted to download or to forward/distribute the text or part of it without the consent of the author(s) and/or copyright holder(s), other than for strictly personal, individual use, unless the work is under an open content license (like Creative Commons).

Disclaimer/Complaints regulations

If you believe that digital publication of certain material infringes any of your rights or (privacy) interests, please let the Library know, stating your reasons. In case of a legitimate complaint, the Library will make the material inaccessible and/or remove it from the website. Please Ask the Library: <https://uba.uva.nl/en/contact>, or a letter to: Library of the University of Amsterdam, Secretariat, P.O. Box 19185, 1000 GD Amsterdam, The Netherlands. You will be contacted as soon as possible.

Chapter 4

Transition from exponential to linear photoautotrophic growth changes the physiology of *Synechocystis* sp. PCC 6803

R. Milou Schuurmans¹, Hans C.P. Matthijs² and Klaas J. Hellingwerf¹

¹: *Molecular Microbial Physiology Group, Swammerdam Institute for Life Sciences, University of Amsterdam, Amsterdam, The Netherlands.*

²: *Aquatic Microbiology, Institute for Biodiversity and Ecosystem Dynamics, University of Amsterdam, Amsterdam, The Netherlands.*

This chapter has been submitted for publication to Photosynthesis Research as:

Schuurmans RM, Matthijs HCP, Hellingwerf KJ. Transition from exponential to linear photoautotrophic growth changes the physiology of *Synechocystis* sp. PCC 6803

Abstract

Phototrophic micro-organisms like cyanobacteria show growth curves in batch culture that differ from the corresponding growth curves of chemotrophic bacteria. Instead of the usual three, i.e. lag-, log- and stationary phase, phototrophs display four distinct phases. The extra growth phase is a phase of linear, light-limited growth that follows the exponential phase and is often ignored as being different. Results of this study demonstrate marked growth-phase dependent alterations in the photo-physiology of the cyanobacterium *Synechocystis* sp. PCC 6803 between cells harvested from the exponential and the linear growth phase. Notable differences are a gradual shift in the binding of the light harvesting phycobilisomes to the photosystems and a distinct change in the redox state of the plastoquinone pool. These differences will likely affect the result of physiological studies and the efficiency of product formation of *Synechocystis* in biotechnological applications. Our study also demonstrates that the length of the period of exponential growth can be extended by a gradually stronger incident light intensity that matches the increase of the cell density of the culture.

Key words:

Batch culture, Biotechnology, Cyanobacteria, Molecular physiology, PSI/PSII ratio

Abbreviations:

PSI, photosystem 1; PSII, photosystem 2; PBS, phycobilisomes; PC, phycocyanin; PQ, plastoquinone; DCMU, 3-(3,4-dichlorophenyl)-1,1-dimethylurea; OD, optical density

Introduction

Successful genetic engineering of cyanobacteria for the synthesis of defined (commodity) products in biotechnological applications, has been amply demonstrated during the past few years [15,17,18,25]. These achievements call for mass cultivation of cyanobacteria; they also initiated this study on the potential growth-phase dependency of the photo-physiological properties of the cyanobacterium *Synechocystis* sp. PCC 6803 (hereafter *Synechocystis*). Different from the general growth pattern of chemoheterotrophic bacteria in batch culture, which is characterized by three successive phases: the lag-phase, exponential growth and stationary phase, respectively, batch growth of phototrophs shows an additional distinctive phase change, i.e. from exponential growth to linear growth. Cell cultures of a phototroph transition from the exponential to the linear phase as soon as the light supply to the culture becomes limiting due to light shading by the increasing number of cells. The typical rate at which photons can be absorbed and processed by the cells (in the sub-ms timescale) is much faster than the half-time of mixing of the culture. Hence, while growing, the cells in a culture are continuously exposed to transitions from light saturation to increasing light limitation. This causes the growth rate to decrease which results in linear growth as soon as cell density increases to values at which all the incident light is absorbed. Finally, additional limitation(s) will kick in, which will cause the cells to enter the stationary phase.

Though, some studies do refer to the phenomenon of a linear growth phase in batch cultures of phototrophic (micro)organisms [228-231], more often the combined period of exponential and linear growth is referred to as cells in the culture being in the log phase, while a linear plot of the increasing OD against time is almost perfectly straight [232].

For cells harvested in the exponential- and in the linear growth phase, differences in mRNA transcript level and protein expression have been reported for genes related to photosynthesis and respiration [233-235]. Significantly, also biofuel production in transgenic cyanobacteria shows variation in product yields during batch growth, with some degree of growth phase dependency [18,236,237]. None of these studies, however, report comparative data on changes in the physiological properties of cells harvested in the exponential and linear phase of growth.

In oxygenic photosynthesis light energy is harvested by antenna pigments and used by photosystem II (PSII) to extract electrons from water; these electrons are transferred through the plastoquinone (PQ) pool via the cytochrome b_6/f complex to photosystem I (PSI), which uses a second quantum of photon energy to allow an electron to reduce NADP^+ . Coupled to the light-driven electron flow, a proton gradient is generated for ATP production. Respiration, which can drive ATP production in the dark, makes use of the same PQ pool in cyanobacteria [99,220]. The largest metabolic sink of the high-free-energy carriers ATP and NADPH is formed by the enzymes of the Calvin Cycle, which jointly catalyze the process of carbon fixation. This requires the light reactions and the so-called 'dark reactions' of photosynthesis (i.e. carbon fixation) to display mutually adjusted rates for optimal supply of ATP and NADPH. To secure sufficient CO_2 availability, cyanobacteria possess an array of CO_2 and bicarbonate transporters [238,239]. When in spite of their presence carbon limitation kicks in, surplus light energy will be wasted as heat and/or fluorescence, which in cyanobacteria involves a range of dedicated proteins associated with the two photosystems, like the orange carotenoid protein (OCP), the flavodiiron proteins and IsiA [122,226,240,241]. Analysis of the dynamical changes in the expression level of the cyanobacterial components involved in energy generation and carbon fixation can give insight into the tuning of both functionally coupled processes.

Light harvesting in cyanobacteria is conducted by membrane bound, non-motile chlorophyll *a* (chl *a*) containing protein complexes coupled to the PSII- and PSI reaction centers, and by the loosely membrane attached and motile phycobilisome antennae complexes (PBS). The PBS can migrate rapidly over the thylakoid membrane surface and transfer energy to either PSII or PSI, or to neither. In the latter case excitation energy is lost as heat and/or emitted as PBS fluorescence [122]. The PBS localization can be monitored by flash freezing of the cells and analysis of the fluorescence emission spectra after specific PBS excitation at 77 K.

PSII-derived fluorescence can be recorded with the non-invasive PAM fluorimetry technique. With low-intensity actinic illumination minimal fluorescence is recorded, while addition of the electron-transfer inhibitor DCMU elicits maximal fluorescence emission. The actually emitted fluorescence from cells incubated under physiological conditions is an indicator for the physiological performance of the cells: The lower the fluorescence the

better [118,204]. The redox state of the photosynthetic machinery can also be determined via rapid extraction of the PQ pool [189]. Regulation of the efficiency of photosynthesis involves both re-distribution of existing light harvesting capacity over the two photosystems through state transitions [242], presumably under control of the redox state of the plastoquinone pool, and by differential gene expression.

In this study we reveal several growth-phase dependent changes of the photo-physiology of *Synechocystis*, harvested in the exponential- and the linear phase of growth. These growth phase dependent adjustments are mostly the result of short-term physiological flexibility, dependent on adaptation mechanisms such as state transitions. Furthermore, the linear growth phase can be prevented or postponed by gradually increasing the incident light intensity, in parallel with the cell density in the growing culture.

Results

Typical growth curve of a batch culture

A typical growth curve of a batch culture of a phototrophic bacterium like *Synechocystis* is schematically depicted in figure 4.1. The figure highlights the transition of exponential growth to linear growth and the slow approach to the stationary phase. Note that the transition to stationary phase can also be more abrupt, and that the data in the left frame is displayed on a log scale, while the right-hand frame has OD on a linear ordinate. These different ways of plotting the data show that the linear growth phase is most clearly displayed in the right-hand frame.

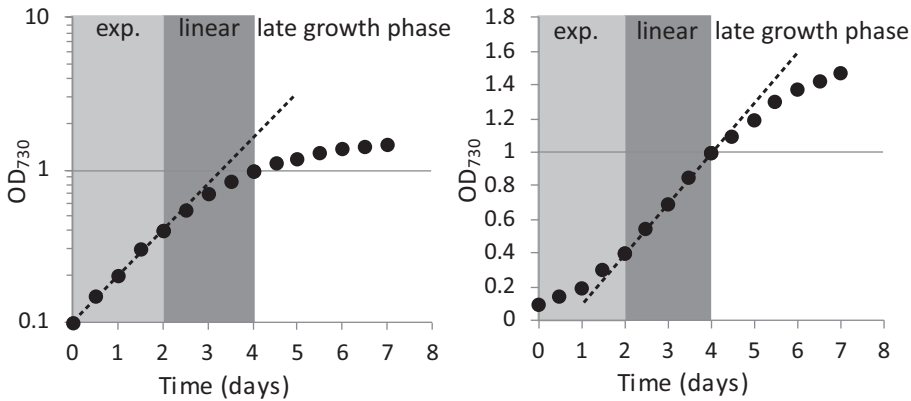


Figure 4.1: Schematic representation of a typical batch culture experiment with *Synechocystis*. Growth conditions: BG-11 medium and moderate incident light intensity. The culture displays an exponential growth phase (exp.), which gradually transits into a linear growth phase, followed by the late- or stationary growth phase.

Gradual changes in chl *a* fluorescence during batch culturing

The effect of the gradually increasing light limitation during batch culturing on the photo-physiology of *Synechocystis* cells was studied by recording several parameters in samples collected during the subsequent growth phases. A representative growth curve is displayed in figure S4.1. For PAM fluorimetry recordings (Fig. 4.2 and Table 4.1) and measurements of the redox state of the plastoquinone pool (Fig. 4.3), samples were dark adapted for 30 minutes, followed by exposure to growth light (GL; $30 \mu\text{mol photons m}^{-2} \text{s}^{-1}$) and then to high light (HL; $300 \mu\text{mol photons m}^{-2} \text{s}^{-1}$). Cells were then returned to darkness, followed by addition of DCMU ($20 \mu\text{M}$) and renewed exposure to growth light. Samples were either used directly from the culture (Fig. 4.2A) or diluted to the uniform OD₇₃₀ of 0.45 (Fig. 4.2B; see Materials and Methods Fig. S4.2 and Fig. S4.3 for further detail). Chl *a* fluorescence recorded from samples that were taken directly from the culture showed a high level of fluorescence quenching at higher cell densities, yielding low fluorescence intensity after a saturation pulse, compared to the values recorded in the presence of DCMU (Fig. 4.2A). To acquire a more informative fluorimeter signal therefore pre-dilution of denser culture samples to OD₇₃₀ = 0.45 was used. This protocol, in which cell density was equalized, permitted comparison of chl *a* fluorescence parameters in all samples regardless of the (cell) density in the culture. Interesting differences can be noticed in the derived numerical data shown in Table 4.1. Cyanobacteria have been reported to emit more fluorescence after

a saturating pulse in the presence of low intensities of actinic light than in darkness [120]. This does not hold for samples taken from the exponential growth phase (OD 0.25 and 0.45); it only becomes apparent in the linear- (OD = 0.8, 1.2 and 1.7) and in the late- (OD = 2.0) growth phase (Fig. 4.2A,B). Also, the calculated apparent photosynthetic quantum yield of PSII (Φ_{PSII} , Table 4.1) appears to increase somewhat with progressing growth phases, and correlates with a decreasing F_0 . The PAM recordings for exponentially growing cells show a weaker response to the light treatments than cells from the linear and late growth phases (Fig. 4.2B). Measured in the presence of an actinic light intensity comparable to incident growth light intensity, the fluorescence increase is stronger, no relaxation response is observed at high light intensities and the dark re-oxidation rate is much lower.

| OD ₇₃₀ | F ₀ | | F _M (dark) | | F _M (GL) | | F _M (DCMU) | | Φ _{PSII} (max) | |
|-------------------|----------------|---------|-----------------------|---------|---------------------|---------|-----------------------|---------|-------------------------|---------|
| | As is | At 0.45 | As is | At 0.45 | As is | At 0.45 | As is | At 0.45 | As is | At 0.45 |
| 0.25 | 159 | 262 | 304 | 501 | 297 | 489 | 299 | 492 | 0.48 | 0.48 |
| 0.45 | 213 | 213 | 438 | 438 | 438 | 438 | 450 | 450 | 0.53 | 0.53 |
| 0.8 | 312 | 204 | 601 | 440 | 628 | 426 | 685 | 437 | 0.55 | 0.54 |
| 1.2 | 342 | 191 | 653 | 417 | 699 | 418 | 752 | 417 | 0.55 | 0.54 |
| 1.7 | 393 | 189 | 761 | 419 | 759 | 435 | 914 | 423 | 0.57 | 0.57 |
| 2.0 | 512 | 195 | 854 | 410 | 870 | 439 | 1197 | 433 | 0.57 | 0.56 |

Table 4.1. Growth-phase dependent changes in chl *a* fluorescence parameters of *Synechocystis*. Variable fluorescence parameters were calculated from duplicate PAM fluorimetry traces as shown in figure 2. The error between traces was < 5 %. Values from both undiluted (as is) and diluted or corrected (at 0.45) PAM recordings are shown. OD₇₃₀, optical density at 730 nm; F₀, minimal fluorescence after dark adaptation; F_M, fluorescence after a saturating pulse in the dark or in growth light intensity (dark, GL), or after addition of DCMU; Φ_{PSII}, yield on PSII ((F_M-F₀)/F_M). Values for Φ_{PSII} are calculated with F₀ and the highest recorded values for F_M (marked in bold).

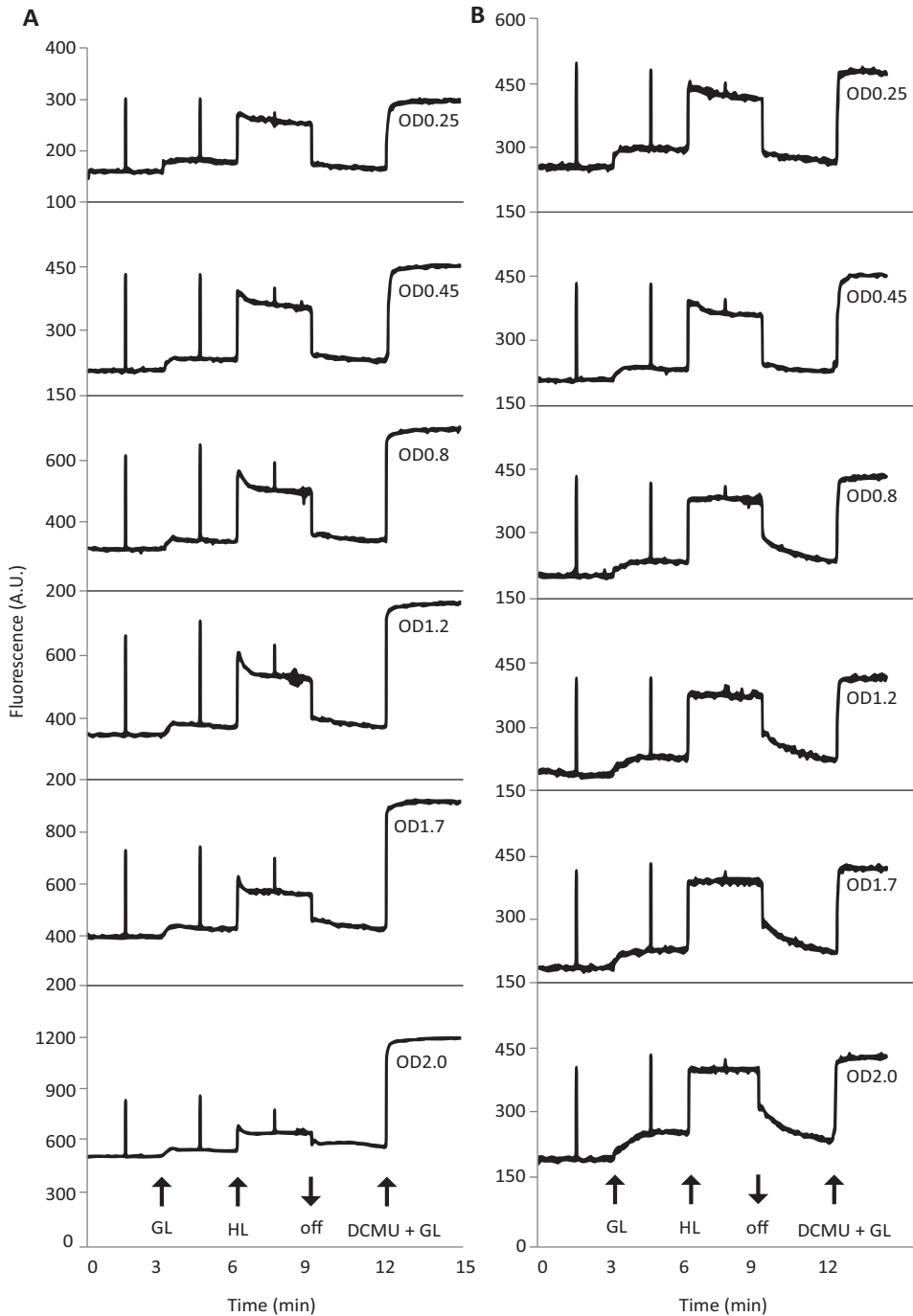


Figure 4.2. Growth-phase dependent changes in chl *a* fluorescence of *Synechocystis*. A. PAM fluorimetry recordings of cells harvested at different growth phases. B. PAM fluorimetry recordings of cells harvested at the same growth phase as in A, but with cells diluted to a standard $OD_{730} = 0.45$; at $OD_{730} = 0.25$ the recording was recalculated to 0.45. GL, growth-light intensity ($30 \mu\text{mol photons m}^{-2} \text{s}^{-1}$); HL, high light intensity ($1000 \mu\text{mol photons m}^{-2} \text{s}^{-1}$); off, darkness; DCMU + GL, DCMU plus growth-light intensity ($30 \mu\text{mol photons m}^{-2} \text{s}^{-1}$).

¹ 655 nm LED light); HL, high-light intensity (300 $\mu\text{mol photons m}^{-2} \text{s}^{-1}$ 655 nm LED light); GL + DCMU, growth light intensity + 20 μM DCMU; asterisk, saturation pulse (2,000 $\mu\text{mol photons m}^{-2} \text{s}^{-1}$ LED light); A.U., arbitrary units. Data displayed are representative recordings.

The plastoquinone (PQ) pool is more reduced in the linear- and late phase of growth

For measurements of the redox state of the PQ pool samples were taken during PAM measurements after dark adaptation and during light treatment in undiluted cultures (see Figs. S4.2 and S4.3 for further detail). At $\text{OD}_{730} = 0.25$ the cell density proved too low for proper redox state analysis. As shown in figure 4.3, the redox state of the PQ pool shifts abruptly from almost fully oxidized in the dark and <20 % reduced in the light in the exponential phase, to about 20 % reduced in the dark and up to 60 % reduced in the light in the linear growth phase. Surprisingly, in the stationary growth phase the redox state appears slightly more oxidized than in the linear growth phase.

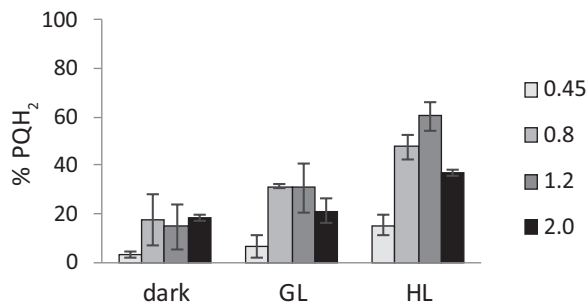


Figure 4.3. Growth-phase dependent changes in the redox state of the PQ pool of *Synechocystis*. Values are in % reduced. GL: growth light intensity (30 $\mu\text{mol photons m}^{-2} \text{s}^{-1}$ 655 nm LED light); HL: high light intensity (300 $\mu\text{mol photons m}^{-2} \text{s}^{-1}$ of 655 nm LED light). The legend specifies the OD_{730} of the culture at the time of sampling. Samples were taken alongside the chl *a* fluorescence recordings depicted in figure 4.2. Error bars indicate the range of variation of a series of duplicate measurements.

Increased binding of PBS to both photosystems in the linear- and the late growth phase

Samples for 77K fluorescence emission analysis were taken directly from the cell culture under growth light intensity (30 $\mu\text{mol photons m}^{-2} \text{s}^{-1}$) and high light intensity (300 $\mu\text{mol photons m}^{-2} \text{s}^{-1}$). For the latter samples the culture was exposed to this high light intensity for 5 minutes. Fluorescence spectra were recorded at 77K with the excitation wavelength set at 590 nm. Figure 4.4 shows that cells collected from the phase of exponential growth display high levels of phycocyanin- (pc, 655 nm) and allophycocyanin (apc, 665 nm)

fluorescence. Furthermore, one can see that as the culture grows more and more dense, PBS fluorescence decreases and PSII- (696 nm) and PSI fluorescence (720 nm) increase. This indicates higher levels of PBS coupling to the two photosystems in the linear and late growth phases. The ratio of the intensity of the different fluorescence signals shows these dynamics in some more detail (Fig. 4.4C,D). The binding of PBS to the two photosystems increases significantly ($pc/PSII$) in the transition from the exponential- to the linear growth phase, with a slight preference for PSII, as reflected by the slight increase in the PSII to PSI fluorescence ratio. Though the total PBS fluorescence decreases, the ratio between pc and apc fluorescence remains stable (pc/apc). On the high-energy side of PSII an additional peak (at 686 nm) is visible. In literature this peak has been attributed to three different proteins: The iron inducible *IsiA* [243], the PSII subunit CP43 [244] and the PBS terminal emitter *Lcm* [245]. The peak at 685 nm shows a similar pattern as the fluorescence peaks for the other PBS sub-units, making *Lcm* the most likely source of this emission.

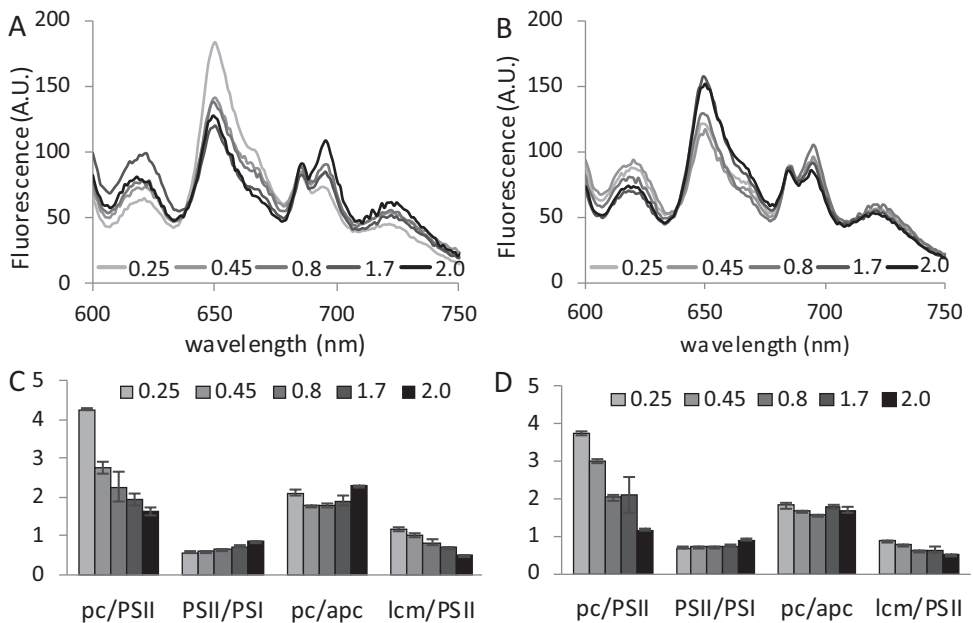


Figure 4.4. Growth-phase dependent changes in light adaptation, as demonstrated with 77K fluorescence emission spectra of *Synechocystis* with 590 nm excitation. Samples were taken alongside the chl *a* fluorescence recordings depicted in figure 4.2. Shown are fluorescence emission spectra at different optical densities taken in growth light (GL, A) and high light (HL, B) conditions, normalized to the area under the curve and the ratios between several peaks at GL (C) and HL (D). Peak area was determined using the peak fitting add-in for excel from

<http://www.chem.qmul.ac.uk/software/eXPFit.htm> on raw data. Peak at: 620 nm, measurement artefact (see Materials and Methods); 655 nm, pc; 665 nm, apc; 686 nm, lcm; 696 nm, PSII; 720 nm, PSI. Data was derived from biological duplicates and technical triplicates; shown is the average with standard deviation.

Protein expression levels of the two photosystems and of the Rubisco enzyme

To test if the physiological changes observed in the photo-physiology of *Synechocystis* could be caused by changes in the level of protein expression of the components of the photosynthetic machinery and/or Rubisco, quantitative Western blotting was used. Cell samples were taken directly from the cell culture and lysed using a French press. Cell-free extracts were analyzed by Western blotting with specific antibodies elicited against PsbA (D1 subunit of PSII), PsaC (a subunit of PSI) and RbcL (large subunit of Rubisco). As an internal standard the levels of AtpB were determined. The levels of the tested proteins barely change in these samples (Fig. 4.5A). In figure 4.5B the average stain density of three separate blots is shown, and from this data a slight downward trend may be observed along with the transition from exponential- to linear growth.

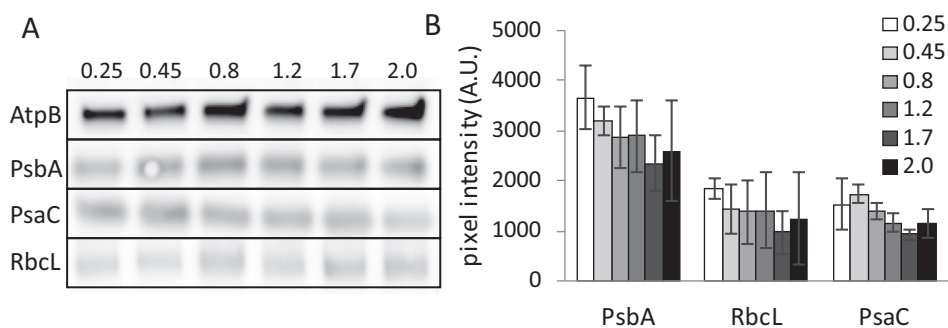


Figure 4.5. Western blots showing expression levels of selected proteins involved in photosynthesis at different growth phases in *Synechocystis*. Samples were taken prior to the chl *a* fluorescence recordings depicted in figure 4.2 at growth light intensity ($30 \mu\text{mol photons m}^{-2} \text{s}^{-1}$) and the legends indicate the optical density at the time of sampling. A. Protein immunoblots showing the content of PsbA, PsaC, RbcL and AtpB in *Synechocystis*. Ten micrograms of total protein were loaded in each lane. B. Pixel intensity of protein immunoblots normalized to AtpB levels. Three individual blots for each protein were analysed with ImageJ; values shown are averages with standard deviation.

Onset and cause of the phase of linear growth

To provide evidence that the linear phase of growth is caused by light limitation only, a batch culture was exposed to light that increased in intensity in parallel to the increasing cell density, to extend the length of the exponential phase (Fig. 4.6, black dots). Diminishing

the decrease in light intensity perceived per cells in this way significantly extends the length of the exponential growth period, to the extent that under the selected conditions the exponential growth phase fully replaces the linear growth phase. By changing the gas-phase of the cultures from CO₂ enriched air to nitrogen only (via bubbling with nitrogen gas) cultures can rapidly be brought to carbon limitation, independent of the light supply. Figure 4.6 shows that cells then instantaneously enter the stationary phase. This experiment shows that the observed transition from exponential to linear growth indeed is caused solely by light limitation.

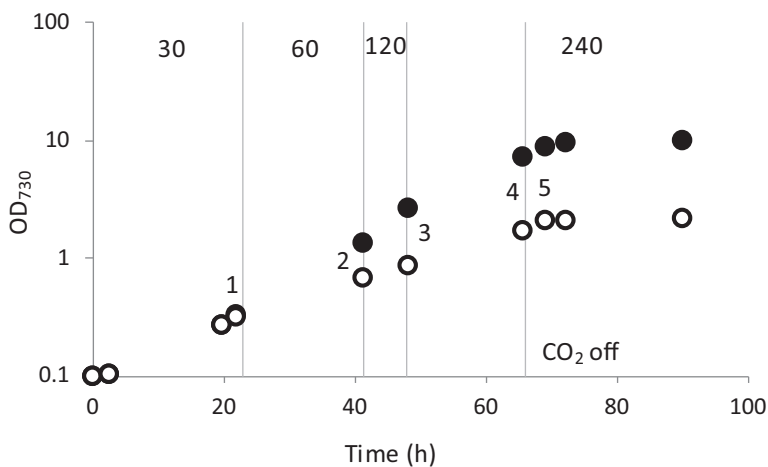


Figure 4.6. Growth curve of *Synechocystis* in BG-11 medium in two illumination regimes with 10 mM TES-KOH pH 8 and air + 1 % CO₂ bubbling. White dots: cultures growing at 30 μmol photons m⁻² s⁻¹. Black dots: cultures growing under increasing incident light intensity conditions as indicated by the vertical grey lines and the light intensity marked at the top in μmol photons m⁻² s⁻¹. Grey dotted line, CO₂ supply stop for all cultures. Shown is the average of four individual batch cultures, the standard deviation was too small to be visible. The numbers in the figure refer to the sampling points at which cells were analysed with qPCR (see Fig. 4.7).

Lower levels of mRNA for carbon uptake systems in the linear growth phase

Here the level of transcription of several carbon uptake systems was investigated, since faster growth will be supported by higher rates of carbon fixation. We chose to test the low C_i inducible ATP-dependent bicarbonate and carbonic acid transporter *cmpA*, the low C_i inducible Na⁺ dependent bicarbonate transporter *sbtA* and *ndhF4*, an NADPH dehydrogenase involved in constitutive CO₂ uptake. For this experiment samples were taken for qPCR from the experiment depicted in figure 4.6. The order of sampling is

depicted in this figure: (#1) before the light intensity was increased, i.e. when all parallel cultures were still subject to the same regime; these samples were used as the reference. Next samples were taken in each illumination condition, just before the conditions were changed (#2, 3 and 4), followed by one last sample in the (intentionally induced) carbon-limited stationary phase (#5). The qPCR results show that the cultures that were enabled to continue exponential growth by raising of the incident light intensity, show little to no (downward) change in the expression levels of the different carbon uptake systems; taking away the CO₂ supply gives rise to a sharp response: Less transcript for the constitutive transporter NdhF4 and more of the inducible transporter CmpA (Fig. 4.7A). In contrast, in the control culture where the light intensity was kept constant and the culture transitioned to linear growth, a consistent decrease in the expression level of the tested carbon uptake systems was revealed (Fig. 4.7B).

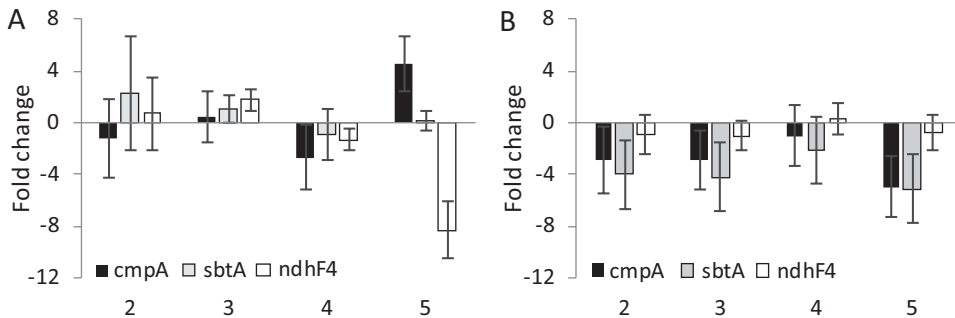


Figure 4.7. Fold change in expression levels of three C_i transporters at different stages of growth in *Synechocystis*, analysed with qPCR. A, changes in expression in cultures growing exponentially at increasing light intensities (black dots in Fig. 4.6) relative to expression levels at the lowest light intensity (#1 in Fig. 6). B, changes in expression in linearly growing cultures at low light intensity (open dots in Fig. 6) relative to the expression levels when growth was still exponential (#1 in Fig. 4.6). *cmpA*, encodes sub-unit of the ATP-dependent HCO₃⁻ transporter; *sbtA*, Na⁺ dependent HCO₃⁻ transporter; *ndhF4*, subunit of the NADPH dependent CO₂ transporter. Expression levels were normalized to the expression of the housekeeping gene *rnpB*. Shown are averages of biological duplicates with the relevant error range.

Discussion

Heterotrophic microorganisms that are grown in batch culture have three distinct growth phases: An optional lag phase, a log phase (also known as the exponential growth phase) in which there is no nutrient limitation, and a nutrient-limited stationary phase in which cells do not or barely grow. Photoautotrophic microorganisms on the other hand display an additional phase known as the linear growth phase, marked by limited and inhomogeneous availability of the substrate light. Proof that decreased light availability is the effector for the transition of the exponential- to the linear growth phase is provided here in an experiment in which, along with cell density, the light intensity was raised, which prolonged the duration of the exponential growth phase and even prevented the transition because those cells directly entered the stationary phase.

Growth-phase dependent changes of gene expression for the cyanobacterium *Synechocystis* sp. PCC 6803 were earlier reported by Foster et al. [235], who observed in a microarray study that the transcript level of almost all genes related to photosynthesis decreases in the linear growth phase. A year earlier it was found that expression level of the *isiA* and *psbA* genes fluctuate during growth with high expression levels in the exponential phase [234]. The present study adds to this that transitions between subsequent phases of growth are actually accompanied by physiological changes affecting photosynthesis. Chl *a* fluorescence, recorded by PAM fluorimetry, showed increased levels of emitted fluorescence in response to light, as growth progressed, accompanied by a decrease in the dark re-oxidation rate of PSII. This indicates slightly higher PSII activity relative to respiratory- and PSI-activity (the two fluxes that oxidize the plastoquinone pool). The question then arises whether the recorded changes resulted from adaptation at the level of transcription or translation rather than that they were based on regulation at the post-translational level. To answer this question we used various analytical techniques: Firstly, 77K fluorescence emission spectroscopy, which provided insight into the positioning of the phycobilisome light harvesting antenna relative to the two photosystems. The data obtained show that functional antenna binding to PSII increased when cell density increased, which connects well to the observed shift of the plastoquinone pool to a more reduced state in the linear growth phase.

Additional insight into possible changes in the expression level of photosynthesis-related proteins was obtained via quantification of some key proteins by quantitative Western blotting analysis, using PsbA for PSII, PsaC for PSI, and RbcL for RuBisCO to survey possible changes in carbon fixation. Though Western blotting revealed that a slight downward trend occurred for the expression level of all proteins tested as growth progresses, their relative decrease was comparable, indicating that there was no change in PSI to PSII reaction center ratio, which could have provided an alternative explanation of the observed reduction of the redox components of the PSII-acceptor side and of the PQ pool.

Analysis of the transcript abundance of several inorganic carbon transporters, i.e. the low C_i inducible *cmpA* [246] and *sbtA* [247] and the constitutive C_i concentration insensitive *ndhF4* [248] revealed that compared to cells in the exponential phase of growth (that do have a higher carbon demand), cells that show linear growth show a decrease in transcript abundance. This implies that a high carbon demand at high growth rates gives rise to a different regulation than the response to low C_i conditions of both inducible and constitutive C_i transporters. Under the carbon-limiting conditions induced here, the expression level of almost all tested carbon uptake systems is lower than in exponentially growing cells. This demonstrates that a higher carbon demand can also have a stronger inducing effect on gene transcription of these uptake systems than under carbon limitation.

An interesting trend in the chl a fluorescence parameters is the increasing apparent photosynthetic yield (ϕ PSII, Table 4.1) as growth progresses. Cultures in the exponential phase have a somewhat higher F_0 value compared to cells from the linear and late growth phase in diluted cultures. 77K fluorescence emission spectra show high levels of PBS fluorescence in the exponential phase, which strongly and continuously decreases in the linear and late growth phases. PAM fluorimetry on cyanobacteria is compromised by several aspects intrinsic to the photosynthetic machinery of cyanobacteria, making PAM data more difficult to interpret in these organisms [249]. The most influential one of these aspects is PBS background fluorescence which causes underestimation of the ϕ PSII by artificially increasing perceived F_0 values [120,249]. The change in ϕ PSII observed here is most likely another example of PBS background fluorescence interference rather than an actual increase in ϕ PSII with decreasing growth rate. A second point of interest is that

cyanobacteria are described to be in state II in the dark, with little binding of the PBS to PSII [120]. In ambient (growth) light the cells then go to state I, with strong binding of the PBS to PSII. As a result of this, saturation pulses given in growth light result in higher levels of chl *a* fluorescence, due to better energy transfer to PSII, than saturation pulses given in the dark [120,182]. Yet in this study we only observe this behavior in the linear and late growth phases ($OD_{730} \geq 1.2$). From 77K fluorescence emission spectra it appears that the proposed state I transition in the light only occurs in the linear and late growth phases, where PBS binding to PSII is strong, while cells in the exponential phase remain in state II, with low levels of PBS binding to PSII and therefore no increase in energy transfer to this photosystem.

The changes in the photo-physiology that are observed in this study appear to be mainly based on adaptation of the antenna to photosystem connectivity. In the exponential phase plentiful light gives rise to photon-energy dissipation as antenna fluorescence, without signs of lesser transcription or expression of phycobilisome proteins. This confirms the expression studies conducted by Singh et al. [234] and Foster et al. [235]. The changes observed in this study in the chl *a* fluorescence response can be explained by the changes in antenna binding and the redox state of the plastoquinone pool, but it does not explain why these changes occur. Cells in the exponential phase are, by definition, light saturated and the rate-limiting step of photosynthesis will then be on the acceptor side of the PQ pool at the point of carbon fixation [250,251]. This means that the rate of input of electrons into the PQ pool should exceed the rate of output, leading to a net reduction of the PQ pool. Yet this does not happen; instead energy transfer to PSII, and therefore PSII activity, is lowered to prevent strong reduction of the plastoquinone pool, and to retain balance between energy production and consumption. This is consistent with our earlier findings that, under carbon limiting conditions, the plastoquinone pool is more oxidized than under carbon replete conditions [189]. But this does not explain why the PQ pool becomes more reduced under light-limited conditions than under light-saturated conditions: One would expect that if ATP and NADPH production are limiting, the PQ pool would remain oxidized. These findings indicate that the conditions on the acceptor side of the PQ pool, such as ATP and NADPH consumption are dominant in determining the rate of energy transfer to PSII, and as a result, the PQ pool redox state.

In recent years the interest in phototrophic microorganisms for biotechnological applications has increased strongly [4,222,252]. Their independence from arable land and the higher photosynthetic yield on light compared to plants, make algae and cyanobacteria ideal candidates for CO₂-based biomass and biofuel production [253]. Improving growth and biomass- or product formation in large scale cultures is a main priority in this field of research. One way to improve growth is to alleviate rate-limiting steps, for instance by increasing the rate of carbon fixation. Work along such lines was reported by Durão et al. [254] via mutagenesis of Rubisco, which indeed led to an increase in the rate of oxygen evolution in the transgenic strains. However, no effect on the maximal growth rate of the engineered cells was observed. Yet the growth curve provided as the basis for this conclusion shows no more than two data points from the exponential phase of growth; the rest of the curve shows linear growth in which light supply rather than carbon fixation was limiting growth. Therefore, it remains to be seen whether this strain, when studied under light-saturated- and nutrient replete conditions, will demonstrate a higher maximal growth rate. This is another illustration that in many studies the exact growth phase of a cell culture matters, both in fundamental and applied research. Several studies with transgenic biofuel-producing cyanobacteria have already shown that product yields and carbon partitioning to product can differ between growth phases [18,236,237]. The variations in product yield over the course of growth in batch can also differ between different products of interest [18,236] and determining the optimal growth phase for harvesting of any particular product could be very helpful in optimizing production and product yield.

Materials and Methods

Strains and culture conditions

Synechocystis sp. PCC 6803 was grown as a batch culture in a photobioreactor [255] at a temperature of 30°C. Growth was in continuous white fluorescent light (30 μmol photons m⁻² s⁻¹ incident light) in BG-11 mineral medium [163] with 10 mM Na₂CO₃. Mixing was established with a stream of sparged air, enriched with 1 % CO₂ at a rate of 20 L h⁻¹. In the experiment where the exponential phase was extended *Synechocystis* sp. PCC 6803 was grown as a batch culture in a multicultivator (PSI) in BG-11 mineral medium with 10 mM

TES-KOH pH 8; the culture was bubbled with 1 % CO₂ enriched air. Growth was in continuous white fluorescent light which was increased manually in parallel to increasing cell density.

PAM fluorimetry

100 ml aliquots of the *Synechocystis* cultures were taken at different times during growth, thus covering different growth phases. At higher cell densities chl *a* fluorescence was recorded from samples as is and from samples that were diluted to an OD₇₃₀ = 0.45 prior to recording. At cell densities below OD₇₃₀ = 0.45, chl *a* fluorescence was recorded as is and recalculated to OD₇₃₀ = 0.45 for the comparison in figure 4.2B. Collected samples were placed in a small flat panel vessel with a light-path of 3 cm. The vessel was placed in between two 660 nm LED light sources to ensure a constant light climate inside the vessel. The culture was mixed by a stream of sparged air, enriched with 1 % CO₂ at a rate of 10 L h⁻¹ and by a magnetic stirring device. The monitoring optical fiber of the PAM-100/103 fluorescence monitoring instrument (Walz, Germany) was placed against the side of the vessel, perpendicular to the light sources. The vessel was equipped with a rapid sampler, used for PQ redox state determination, as well as a syringe with a long needle for rapid DCMU addition (see Fig. S4.2 for a schematic of this set-up). At the start of the experiments the cultures were dark-adapted for 30 minutes, after which the cultures were exposed to 3 minutes of illumination at growth light intensity (30 μmol photons m⁻² s⁻¹), followed by 3 minutes of illumination at high light intensity (300 μmol photons m⁻² s⁻¹). At 1.5 minutes before the light conditions changed a saturation pulse (2,000 μmol photons m⁻² s⁻¹), generated by the same LED lamps that secured the actinic light, was applied to determine F_M. After the light treatments the culture was incubated in the dark for 3 minutes followed by a final treatment with 20 μM 3-(3,4-dichlorophenyl)-1,1-dimethylurea (DCMU, Sigma) at growth light intensity (see Fig. S4.3 for a schematic representation of this regime).

PQ pool redox state measurements

Samples for the determination of the PQ pool redox state were taken during the PAM fluorimetry experiment, as described above and indicated in figure S4.3. Samples were taken shortly before application of the saturating pulse in the dark-adapted state and during growth-light- and high-light illumination. During dark adaptation, before chl *a*

fluorescence measurements, samples were taken and fully reduced with NaBH₄ to determine the size of the PQ pool. For plastoquinol (PQH₂) extraction, detection and subsequent PQ pool redox state analysis the method as described earlier in Schuurmans et al. [189] was used. In short, samples were quenched in an ice-cold mixture of 1:1 (v/v) methanol/petroleum ether (PE), followed by vortexing and centrifugation. The top PE phase was transferred to an N₂-flushed glass tube and the PE extraction was repeated. PE phases were pooled and dried under a continuous stream of N₂ gas. Dried samples were re-suspended in hexanol and the PQH₂ was detected using HPLC with fluorescence detection (excitation/emission was set at 290/330 nm). The PQ pool redox state was calculated using the PQH₂ values obtained from fully (NaBH₄) reduced samples as a 100 % reference.

77K fluorescence emission analysis

For 77K fluorescence analysis samples were taken at different growth phases and diluted to a final OD₇₃₀ of 0.15 in BG-11 medium with glycerol (final concentration 30 % (v/v)) and immediately frozen in liquid nitrogen. The samples were analyzed in an OLIS 500 spectrofluorimeter, equipped with a Dewar cell. This fluorimeter always generates a peak within the first 50 nm of the recorded emission spectra, irrelevant of the excitation wavelength or the start of emission spectra acquisition. Because this phenomenon is consistent and independent of the sample conditions it has been deemed an artifact, in this study the artifact is visible at 620 nm. PBS-specific excitation light was used at 590 nm, and fluorescence emission spectra were recorded between 600 and 750 nm, a wavelength domain in which the phycobilisomes (655 nm, pc and 665 nm, apc), PSII (696 nm), and PSI (720 nm) show well-separated emission peaks. Peak de-convolution was performed using the peak fitting add-in for excel from the site: <http://www.chem.qmul.ac.uk/software/eXPFit.htm> on the different peaks, in order to assay the degree of coupling of the PBS to PSII and PSI.

Western blotting

Cell samples were taken from the *Synechocystis* culture at different growth phases to a final OD₇₃₀ of 60 in 1 ml. Samples were spun down (10 min, 3500 g) and resuspended in 50 mM MES buffer, pH 6.5. The cells were broken by four passages through a French pressure cell at 12,000 p.s.i. The protein concentration of the cell free extracts was determined with a

Pierce BCA assay and 10 µg of protein was loaded onto 15 % SDS-PAGE gels. Gels were run for 2 hours at 10 mA per gel and proteins were transferred to nitrocellulose membranes by wet blotting at 50 mA overnight. Blots were stained with antibodies elicited against AtpB and PsbA or PsbC. Blots with antibodies against RbcL were conducted without AtpB because these proteins are of approximately the same size. For each antibody at least 3 blots were made. GARPO (goat-anti-rabbit-peroxidase) was used as the secondary antibody. Visualization was achieved using a supersensitive chemo-luminescence kit (Thermo) and a LiCor Odyssey FC Imager. Band intensity was determined in triplicate using ImageJ software. Band intensities of the different proteins were normalized to the band intensity of AtpB. RbcL band intensity was normalized to AtpB from AtpB-PsbA blots which were conducted simultaneously.

Transcript analysis by qRT-PCR

Synechocystis cells were harvested at the different time points indicated in figure 4.6, and rapidly concentrated to a uniform final OD₇₃₀ = 3.3 in 1 ml and opened by bead-beating with intervals for cooling, cell debris was removed by centrifugation. Prior to use, the glass beads were washed in 4N HCl and ethanol and autoclaved twice. RNA was isolated using the RNeasy mini kit (Qiagen) and further used to prepare cDNA with the RevertAid First Strand cDNA 13 Synthesis Kit (Thermo Scientific). RNA quantity was determined on a Nanodrop 1000 spectrophotometer (Thermo Scientific) and quality assessed on a 1 % agarose gel to confirm RNA integrity. For cDNA formation the RevertAid First Strand cDNA Synthesis Kit (Thermo Scientific) was used with the M-MuLV Reverse Transcriptase and random hexamer primers. The cDNA yield was analyzed by qRT-PCR in an Applied Biosystems 7300 Real Time PCR system using the Power SYBR® Green PCR Master Mix (Life Technologies) employing gene specific primers. Gene specific primers were designed with Primer3 software (Life Technologies) (Table S4.1) for the ATP dependent HCO₃ transporter sub-unit *cmpA*, the Na⁺ dependent HCO₃ transporter *sbtA*, the NADPH dependent CO₂ transporter sub-unit *ndhF4* and the housekeeping gene *rnpB* [256]. The relative abundance was calculated and normalized to *rnpB* which is used as a housekeeping control [256] in samples from different conditions or different mutant strains.

Acknowledgements

We would like to thank Merijn Schuurmans and Angie Vreugdehil for their help with the experimental procedures.

Supplemental Material

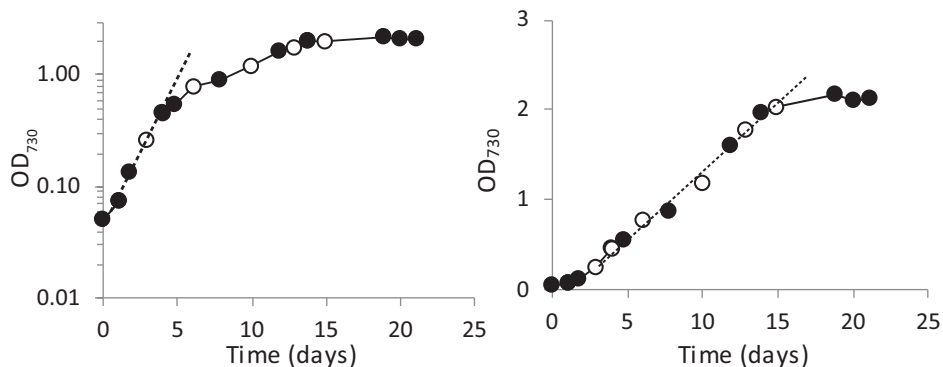


Figure S4.1: Batch culture sampling scheme. Growth curve of *Synechocystis* WT growing in batch with incident white light at $30 \mu\text{mol photons m}^{-2} \text{s}^{-1}$ in BG-11 medium with 10 mM Na_2CO_3 , bubbled with air + 1 % CO_2 at 30 °C. The open circles indicate the time points at which samples were taken for further measurements, at the closed circles only the optical density was measured.

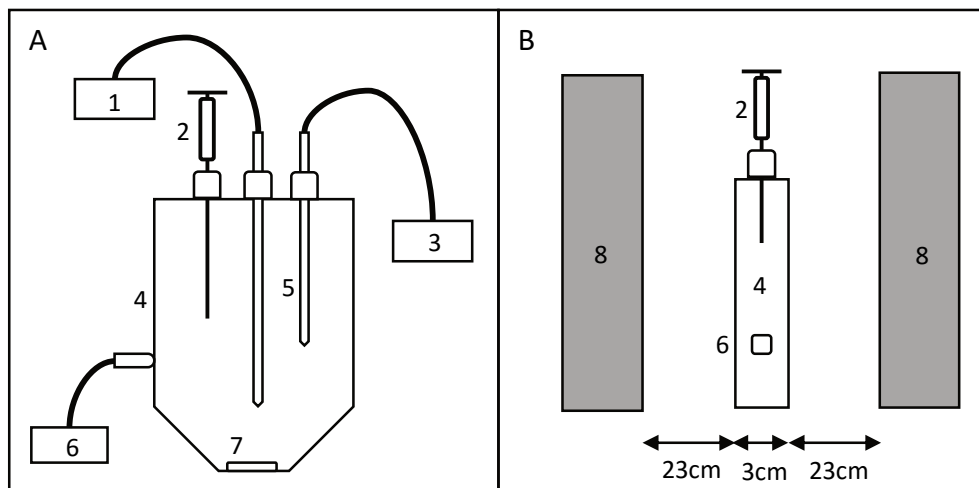


Figure S4.2: schematic representation of the PAM-set-up. A: front view; B: side view. 1, inlet for 1 % CO_2 enriched Air supply ($10 \text{ L}\cdot\text{h}^{-1}$); 2, Syringe; 3, Rapid sampler; 4, Flat panel vessel; 5, Hollow glass rods; 6, location of the PAM light guide fiber; 7, Stirring magnet; 8, LED panels.

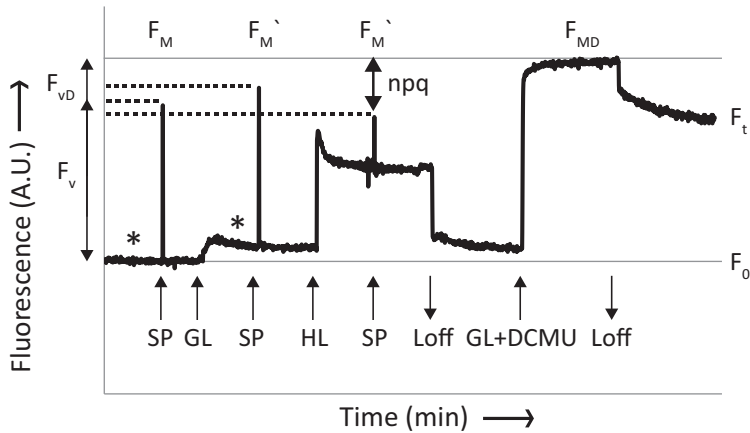


Figure S4.3: Schematic representation of results of measurement of variable chl *a* fluorescence. Typical example of a chl *a* fluorescence trace of *Synechocystis* as acquired in this study. SP, saturating pulse; GL, growth intensity actinic red light ($30 \mu\text{mol photons m}^{-2} \text{s}^{-1}$); HL, high actinic red light ($300 \mu\text{mol photons m}^{-2} \text{s}^{-1}$); L_{off}, actinic light is switched off; GL+DCMU, $30 \mu\text{mol photons m}^{-2} \text{s}^{-1}$ red light + $20 \mu\text{M DCMU}$. F_t , fluorescence level at any given time; F_0 , fluorescence level in the dark; F_M , level of fluorescence acquired with a saturating pulse in the dark; F_M' , level of fluorescence acquired with a saturating pulse in the light; F_{MD} , level of fluorescence acquired in the presence of DCMU and GL. F_v , variable fluorescence ($F_M - F_0$); F_{vD} , variable fluorescence ($F_{MD} - F_0$); npq, non-photochemical quenching. Stars, sampling points for determination of the PQ redox state.

| Name | Sequence 5' - 3', forward primer | Sequence 5' - 3', reverse primer |
|--------------|----------------------------------|----------------------------------|
| cmpA | ATCCTGACACCGATATTGACCTACT | CGCATGCCCTGGACTGTT |
| sbtA | CCGGAAGATAATCGGGTCAA | GGCAGGGCCTTGAAACTTCT |
| ndhF4 | CCCCATTTTCAGTGATATTTTGA | TGTTATTTATGAGCATTGGTTCGATT |

Table S4.1. Primers used for qPCR analysis.